

Influence of the substrate type on the microstructural, optical and electrical properties of sol–gel ITO films

L. Predoana · S. Preda · M. Nicolescu ·
M. Anastasescu · J. M. Calderon-Moreno ·
M. Duta · M. Gartner · M. Zaharescu

Received: 23 January 2014 / Accepted: 21 April 2014 / Published online: 7 May 2014
© Springer Science+Business Media New York 2014

Abstract Indium tin oxide (ITO) is recognized as the best transparent and conductive material [transparent conducting oxide (TCO)] until now and its properties are dependent on the preparation method. In the present work ITO films with In:Sn atomic ratio 9:1 were prepared by a sol–gel route on different substrates (microscope glass slides, microscope glass covered with one layer of SiO₂ and Si wafers) for TCO applications. The multilayer ITO films were obtained by successive deposition by the dip-coating method and the films were characterized from the structural, morphological, optical, and electrical points of view using X-ray diffraction, scanning electron microscopy, atomic force microscopy, spectroscopic ellipsometry and by Hall effect measurements, respectively. The results showed that the thickness, optical constants and carrier numbers depend strongly on the type of substrate, number of deposited layers and sol concentration. The optical properties of ITO films are closely related to their electrical properties. The enhancement of the conductivity was possible with the increase of crystallite size (which occurred after thermal treatment) and with the reduction of surface roughness.

Keywords ITO film · Sol–gel process · Microstructure, optical and electrical properties

1 Introduction

Indium tin oxide (ITO) is an important material as it is one of the most widely used transparent conducting oxides (TCOs) required as a component in photovoltaic cells [1, 2], electroluminescent devices [3], transparent electrodes in plasma display panels [4], sensor modules [5], protective coatings [6] and so on.

Properties required for TCOs are low resistivity (as $1.0 \times 10^{-4} \Omega \text{ cm}$), conductivities higher than 10^3 S/cm , low extinction coefficient k in the optical visible (Vis) spectral range, wide band gap ($E_g > 3.0 \text{ eV}$) that ensure the transparence in visible range and optical transmittance higher than 80 %.

In order to ensure the required properties of the transparent conductive oxides, several methods of preparation were used, such as: sputtering [7–15], spray pyrolysis [16–18], screen printing [19, 20], ion beam assisted deposition [21, 22], microwave [23], evaporation [15, 24, 25] and sol–gel [26–33]. More recently, ITO nanocrystals have been synthesized by hydrothermal process followed by annealing at 450 °C in forming gas for 1 h [34]. The post densification reducing thermal treatment in forming gas was performed to decrease the resistivity of the ITO films by a factor of two [19, 34].

The sol–gel method presents some interesting advantages over other methods of coatings deposition, such as: easy control of the final materials, the possibility of deposition on complex shaped substrates, easy control of doping concentration, structural homogeneity, low temperature of thermal treatment of films, as well as the low cost equipments.

In the present work indium thin oxide transparent films with In:Sn atomic ratio of 9:1 were deposited by a sol–gel route on several substrates: microscope glass, microscope

L. Predoana · S. Preda · M. Nicolescu · M. Anastasescu (✉) ·
J. M. Calderon-Moreno · M. Duta · M. Gartner · M. Zaharescu
“Ilie Murgulescu” Institute of Physical Chemistry, Romanian
Academy, 202 Splaiul Independentei, 060021 Bucharest,
Romania
e-mail: manastasescu@icf.ro

glass covered with one layer of SiO₂ (prepared also by sol-gel method) and Si wafers.

The interest to study the influence of the substrate on the ITO films properties is important for their application as solar cells but also for their newer applications as sensors or protective coatings [5, 6].

The ITO films obtained by sol-gel method were characterized from the morphological, optical, and electrical points of view and the results showed that all physical properties depend strongly on the type of the substrate, solution concentration and number of layers.

2 Experimental

2.1 Solution preparation and film deposition

ITO films with In:Sn atomic ratio 9:1 were prepared as follows: indium nitrate was used as In₂O₃ source, 2 tin ethylhexanoate as SnO₂ source and 2,4-pentanedione as chelating agent, in ethanol solvent.

The composition of the initial solution and the experimental conditions for obtaining sol-gel ITO films are based on the previous published results [27, 29]. Solutions with 0.1 and 0.25 M concentrations were investigated (denoted from here on as 0.1 and 0.25 M ITO). The following molar ratio of the reagents were used: In:Sn = 9:1 and In:EtOH:2,4-pentanedione = 1:35:0.05 for 0.1 M and In:EtOH:2,4-pentanedione = 1:14:0.05 for 0.25 M solutions.

1. Before deposition the viscosity of the solutions was measured with the Brookfield Viscometer DV-II + Pro equipment at room temperature in 8 ml of solution. As expected, the viscosities of solutions show higher values when their concentration is higher (1.37 for the 0.1 M ITO sol and 1.47 for the 0.25 M ITO sol).
2. From the solution prepared as presented above, films were deposited on glass, glass covered with SiO₂ layer (prepared by sol-gel) and Si wafer substrate by dip-coating method with a withdrawal rate of 5 cm/min. Before deposition, the solutions were aged for 24 h. For multiple depositions, after each deposition an intermediary thermal treatment of densification at 260 °C for 10 min, using a heating rate of 5 °C/min, was used. After the last deposition the films were thermally treated at 400 °C for 2 h in air, using a heating rate of 5 °C/min.

2.2 Film characterization

The crystallinity of the sol-gel ITO films was studied by X-ray diffraction (XRD) method. The measurements were

performed using Rigaku Ultima IV equipment, with Cu K α radiation and a fixed power source (40 kV and 30 mA). The diffractometer was set in condition of grazing incident X-ray diffraction (GIXRD) with $\omega = 0.5^\circ$. The mean crystallite size was evaluated from the line broadening of (222) XRD line of ITO thin films using Scherrer's equation: $D = 0.94\lambda/\beta\cos\theta$, where $\lambda = 1.54 \text{ \AA}$ is the X-ray (CuK α) wavelength, θ the diffraction angle, β the full width at half maximum of the (222) diffraction line and 0.94 is the Scherrer constant.

Systematic information on the ITO films morphology and thickness was obtained by scanning electron microscopy (SEM) analysis using a FEI Quanta 3D microscope operating at 5 kV.

Atomic force microscopy (AFM) measurements were carried in the non-contact mode, with a XE-100 apparatus from Park Systems, using sharp tips (highly doped-Si material, <8 nm tip radius; PPP-NCHR type from NanosensorsTM). The topographical 2D and 3D AFM images were taken over the area of $2 \times 2 \mu\text{m}^2$; for displaying purpose and subsequent statistical data analysis [including the calculation of the root mean square (RMS) roughness] XEI (v.1.8.0) Image Processing Program developed by Park Systems was used.

Ellipsometric measurements were performed in order to obtain the thickness and optical (dielectric) constants with J.A. Woollam Co., Inc equipment composed of a rotating-analyzer VASE ellipsometer for UV-VIS-NIR range. Measurements have been performed at room temperature, using 70° as incidence angle with 10 nm wavelength step. The film thickness and the refractive index (*n*) were obtained from the ellipsometric data analysis with an accuracy of $\pm 0.2 \text{ nm}$ and ± 0.005 respectively. The optical transmission measurements were performed at 0° incidence angle on the same apparatus.

Electrical measurements based on Hall effect, were performed on a HMS-5000 equipment from Ecopia using van der Pauw method.

3 Results and discussion

In the experimental conditions presented above, films up to ten layers could be obtained using the solution with 0.1 M concentration, while only five layers could be deposited in the case of the solution with 0.25 M concentration, because it gellified due to its higher viscosity.

The different substrates used for films deposition were selected taking into account the application of the considered films, such as: solar cell [1–4] sensors [5] or protective coatings [6].

The SEM images of the films obtained from 0.1 to 0.25 M sol concentrations and after ten and five layers,

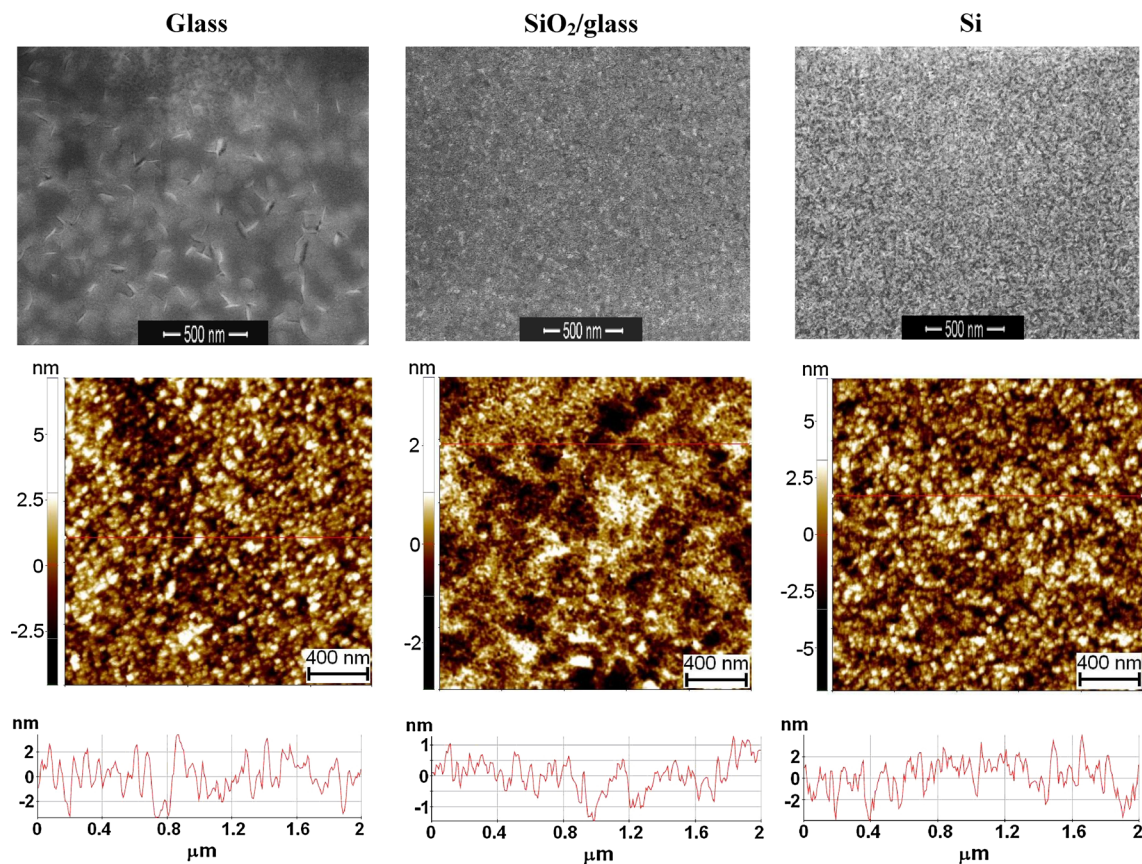


Fig. 1 SEM–AFM comparison for the 0.1 M ITO films with ten layers on glass, SiO₂/glass and Si; *last row* characteristic line-profiles taken from AFM images with *vertical scale* of few nm

respectively, are presented in Figs. 1 and 2 in comparison with AFM images at the same scale. The sol concentration has an important effect on the film microstructure: the higher viscosity leads to coarser features, including roughness and pore size, confirmed by the AFM line profiles (Figs. 1, 2).

The thicknesses of the ITO films were determined by SEM measurements of the films seen edge-on (Fig. 3). The measured thicknesses of the 0.25 M ITO films deposited on glass, SiO₂/glass and Si substrates are: 65 ± 15 , 200 ± 20 and 90 ± 10 nm, respectively. The SiO₂ layer deposited on glass can also be observed in the SEM micrograph in Fig. 3, with a thickness of 50 ± 5 nm. The local variations of thickness are due to the roughness of the films. The ITO film deposited on Si shows the smoothest surface and also the smallest variation in thickness along the film, while the thickest film with the roughest surface have been observed for the film deposited on the SiO₂/glass substrate. The film deposited on glass is the thinnest but its roughness is close to the films deposited on SiO₂/glass substrates.

Figure 4 shows SEM micrographs of the edge of two ITO films deposited on SiO₂/glass substrate: 0.1 M ITO with ten layers and 0.25 M ITO with five layers. The sol

concentration clearly has a strong influence on the thickness. For the 0.1 M ITO sample, the film thickness is barely distinguishable from the SiO₂ film and it is not higher than ~ 20 nm, while it is ~ 200 nm for 0.25 M ITO film after five depositions. The presence of pores with several hundreds nm diameter is also observed in the 0.25 M ITO films after five depositions. The coarse porosity is observed only for films with more than two layers, on the samples prepared with sol concentration 0.25 M, especially on the glass and SiO₂/glass substrates.

Atomic force microscopy measurements revealed the effect of the overall RMS roughness of layer deposition for the 0.25 M ITO films (Fig. 5), showing the effect of the formation of coarser features on the film surface. The RMS roughness increases with the number of depositions almost linearly for 1–5 layers on Si substrate and changes abruptly for SiO₂/glass and glass substrate (three times larger than on Si substrate) after five layers deposition, due to the formation of wider surface cavities (in the range of hundreds nm diameter)—Fig. 5. The roughness of the bare substrates is similar for Si and SiO₂/glass (even <1 nm at 2×2 nm²) and ~ 2 nm (at 2×2 nm²) for the glass explaining the slightly higher roughness values obtained

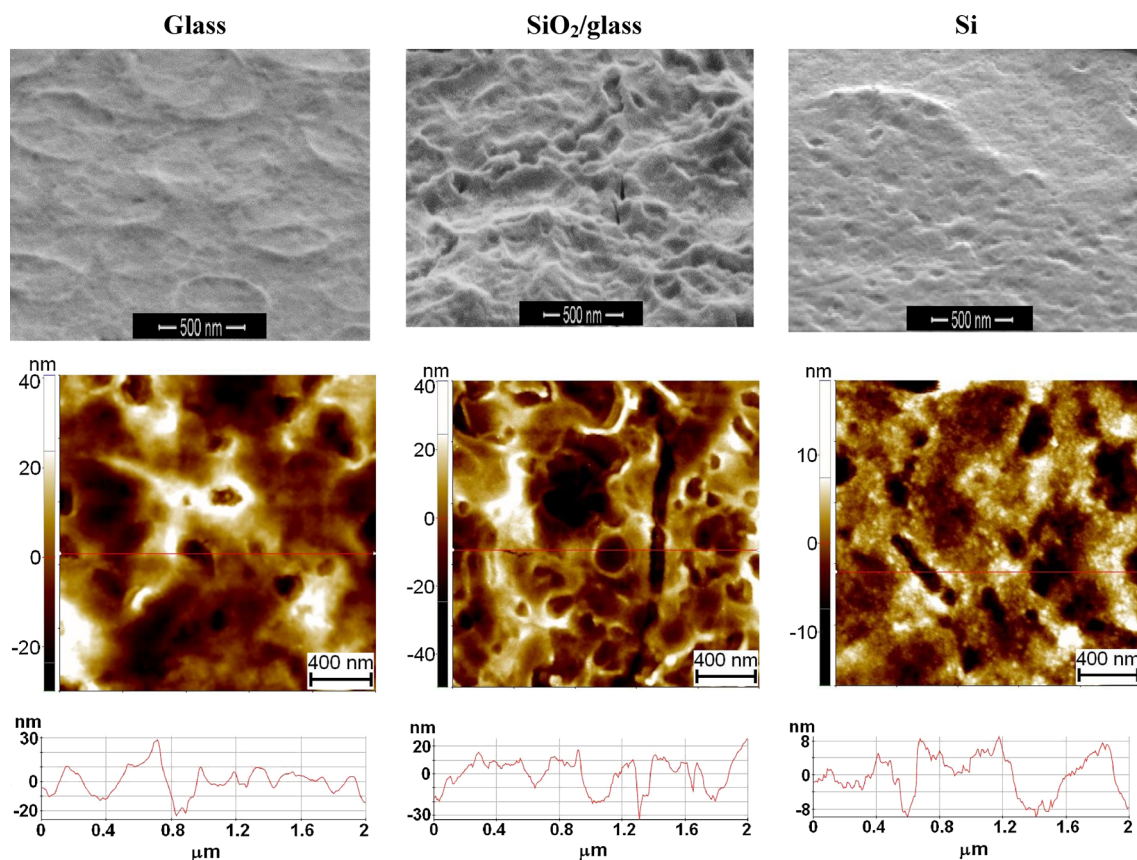


Fig. 2 SEM–AFM comparison for the 0.25 M ITO films with five layers on glass, SiO₂/glass and Si; *last row* characteristic line-profiles taken from AFM images with *vertical scale* of few tens of nm

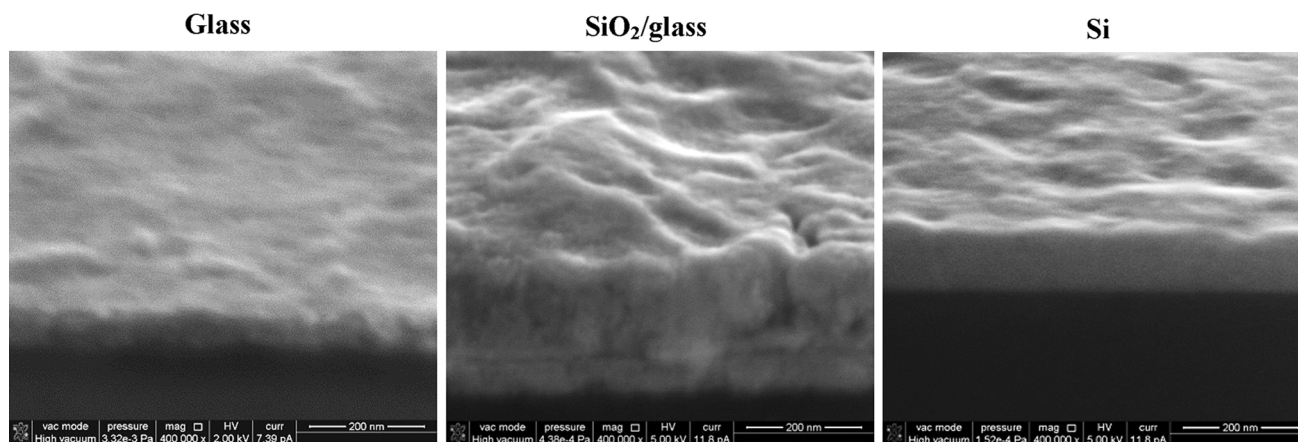


Fig. 3 SEM micrographs of the edge of the 0.25 M ITO films with five layers on glass, SiO₂/glass and Si

after deposition of 1–2 layers of 0.25 M ITO on glass substrate—Fig. 5. On the other hand, the large pores formed after five layers deposition on Si are flattened (around 10 nm deep) as compared to the superficial pores formed on glass (~20–25 nm deep) or SiO₂/glass (~25–30 nm deep) substrates—Fig. 2—and could explain

the roughness behavior observed in Fig. 5 for multilayered 0.25 M ITO films.

The structural characterization of the nanocrystalline ITO films demonstrates that an important parameter during film synthesis is the concentration (and viscosity) of the solution. Low concentration of 0.1 M ITO results in films

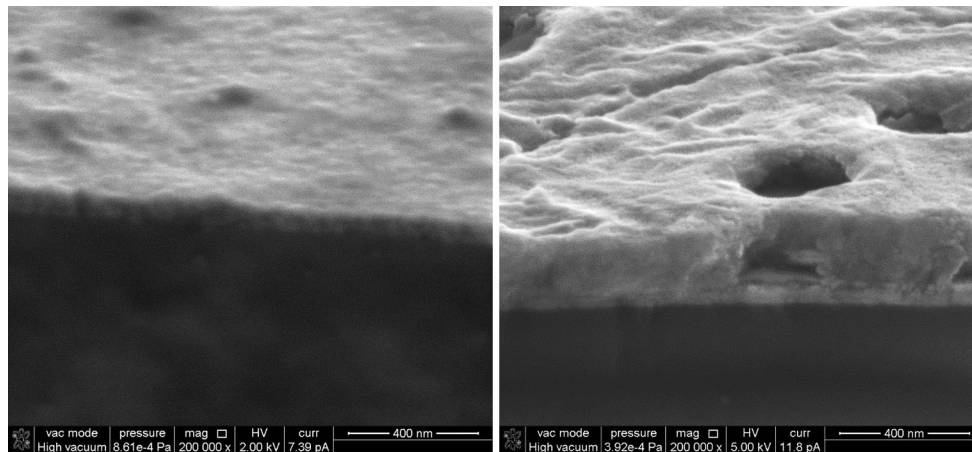


Fig. 4 SEM micrographs of the edge of the ITO films deposited on SiO₂/glass (0.1 M with ten layers and 0.25 M with five layers)

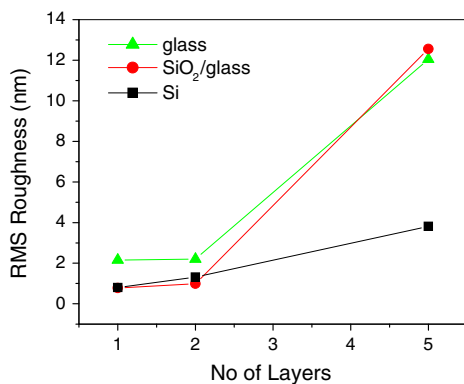


Fig. 5 Roughness dependence on the number of layers for the films prepared from 0.25 M sol concentration (at the scale of $2 \times 2 \mu\text{m}^2$)

with similar thicknesses after ten layers deposition (Table 1) between 22 and 31 nm and reduced roughness (line profiles with vertical scale of ± 2 nm, Fig. 1), for all three substrates. This shows a small effect of the substrate on the successive densification of each 0.1 M ITO layer during thermal treatments. Good wetting of the substrate by the solution leads to the formation of a homogeneous,

continuous layer after the first few depositions and thermal treatments.

We can estimate, from XRD measurements (presented further), that the thicknesses of the ten layers 0.1 M ITO films approximates the size of three ITO crystallites for glass and Si substrates, and ~ 3.7 for SiO₂/glass. The last mentioned substrate induced the thickest films because it is the most reactive one due to the presence of SiO₂ sol–gel layer.

A concentration of 0.25 M ITO leads to significantly thicker films and the formation of coarse porosity. The higher viscosity of the solution hinders the formation of a continuous, homogeneous layer during the first deposition and can promote film growth in the direction perpendicular to the substrate surface, leading to the formation of thicker films and coarser pores.

We can conclude that perpendicular growth of the 0.25 M ITO films after five layers deposition depends significantly on the reactivity of the substrate with the solution: it is significantly lower—around 80 ± 15 nm—on highly stable, dense, non-reactive surfaces, such as those of glass and Si, than in the case of SiO₂/glass substrate— 200 ± 20 nm—(Fig. 3).

Table 1 Electrical parameters: carrier concentration- N_D , resistivity- ρ , mobility- μ , determined by Hall measurements function of molar ITO concentration and the number of layers together with the thicknesses (d_{film}) of ITO films determined by SE measurements

Substrate	Molar concentration of ITO sol (M)	Number of layers	N_D (cm^{-3})	ρ (Ω cm)	μ (cm^2/Vs)	d_{film} (nm) SE	d_{film} (nm) SEM
Glass	0.1	10	1.20×10^{20}	8.74×10^{-2}	0.6	22.1	–
	0.25	5	4.03×10^{17}	5.75×10	0.3	78.5	65
SiO ₂ /glass	0.1	10	3.95×10^{20}	7.81×10^{-2}	0.2	31.1	–
	0.25	5	7.50×10^{15}	1.65×10^2	5.1	205.4	200
Si	0.1	10	4.32×10^{19}	2.98×10^{-1}	0.5	27.3	–
	0.25	5	3.17×10^{18}	4.75×10^{-1}	4.1	92.1	90

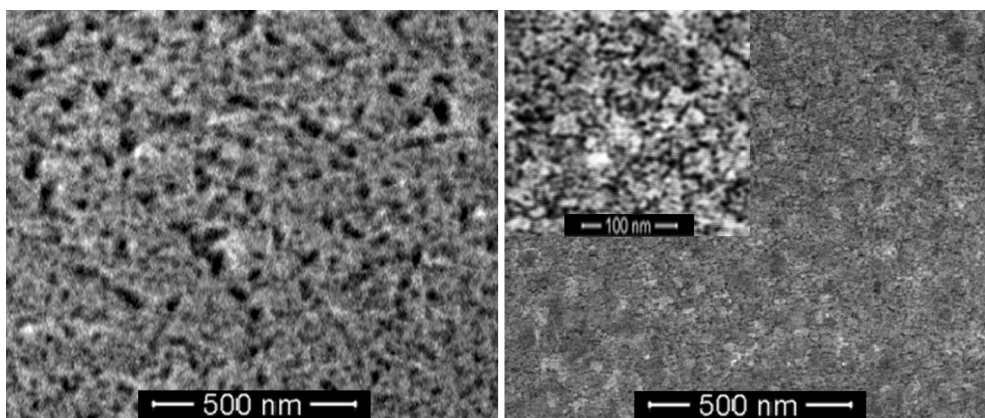


Fig. 6 High resolution SEM micrographs of the surface of the 0.1 M ITO films deposited on SiO₂/glass: with two layers (*left*) and ten layers (*right*), shown at higher magnification in the inset. The *black spots* on the micrographs are pores

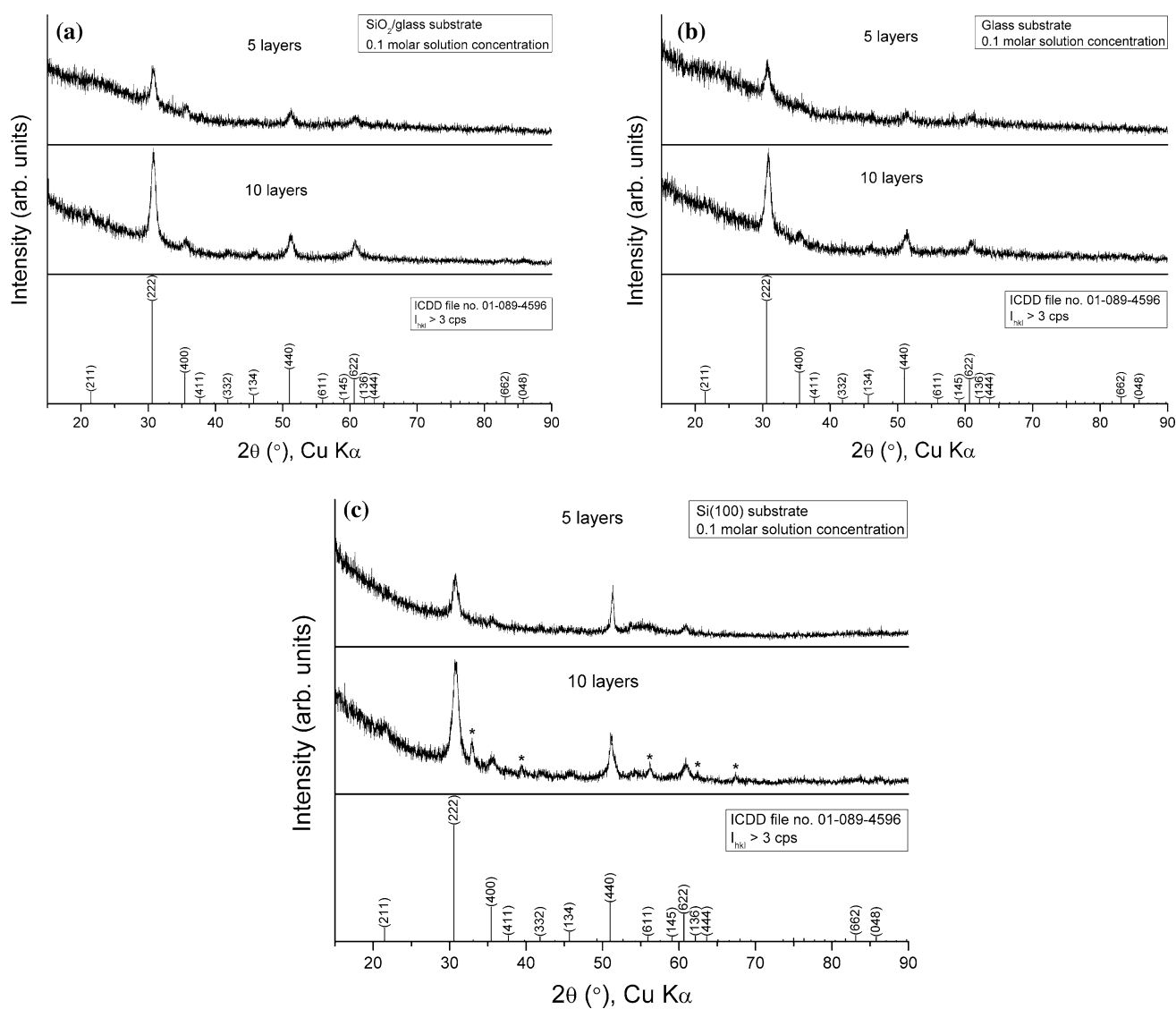


Fig. 7 X-ray diffraction patterns of 0.1 M ITO films on the following substrates: **a** SiO₂/glass, **b** glass and **c** Si(100) (*asterisk* peaks from metallic In used as electrode contacts for electrical measurements)

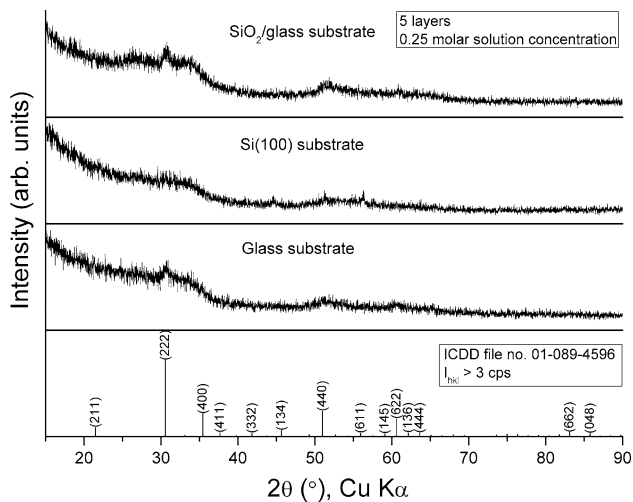


Fig. 8 X-ray diffraction patterns of 0.25 M ITO films deposited on $\text{SiO}_2/\text{glass}$, $\text{Si}(100)$ and glass substrates

Multiple layers deposition has a high contribution in the reduction of pore size. The high resolution SEM micrographs (Fig. 6) show the effect of multiple layers deposition in the nanoscale intrinsic porosity of the 0.1 M ITO samples on $\text{SiO}_2/\text{glass}$, after two and ten layers. There is a clear reduction of the pore size at the nanoscale. For films with two layers, pore sizes of 20–30 nm are observed, while for films with ten layers only much smaller pores are visible (between 5 and 10 nm), as it is shown in the inset of Fig. 6. The same effect of additional layers deposition on nanoscale porosity has been observed on all studied substrates. We attribute the reduction in pore size to their filling with solution by subsequent depositions and to the densification of the films during thermal treatments carried out after each deposition. The reduction in porosity seems to be associated to the observed increase of carrier concentration and lower resistivity after multiple depositions, discussed below.

X-ray diffraction results are presented in Fig. 7 for 0.1 M ITO and Fig. 8 for 0.25 M ITO films annealed at 400 °C. They are polycrystalline and have monophasic cubic bixbyite structure [35] as can be assigned from ICDD file no. 01-089-4596. Diffraction lines are more or less intense following the crystallization degree of the sample when compared to bixbyite structure. The film exhibits the reflection from the (222) plane as the most predominant peak in the XRD pattern, but no preferred orientation can be noticed. None of the patterns present any characteristic lines of tin oxides phases, which indicates that the tetravalent Sn^{4+} replaces In^{3+} substitutionally into the indium oxide lattice, retaining the In_2O_3 structure. For 0.1 M ITO films deposited on all substrates the XRD patterns show a

similar intensity of the diffraction lines indicating a close degree of crystallinity.

For the above-mentioned films, the substrate influences the crystallite size and the unit cell parameters of the crystal structures. The crystallite size values are 9.7 ± 3.3 nm for the films deposited on glass, 10.6 ± 0.3 nm for the films deposited on $\text{SiO}_2/\text{glass}$, and 9.3 ± 0.3 nm for the films on $\text{Si}(100)$. The lattice constant, a , of the cubic structure is 10.0788 ± 0.0005 Å for crystals grown on glass, 10.1068 ± 0.0003 Å for crystals grown on $\text{SiO}_2/\text{glass}$ and 10.0925 ± 0.0002 Å crystals grown on $\text{Si}(100)$.

A vitreous material is not completely random. There are atoms organized in isolated structures where the interatomic distances are approximately constant [36]. This short distance ordering is detected as a single or few broad “diffusion lines” on the diffraction pattern. These lines correspond to the interference of atoms positioned more often at the representative distance, d [37].

On the thin films starting from 0.25 M solution, the X-rays diffraction lines have low intensities, even after five depositions and subsequent thermal treatment and only a broad line corresponding to the (222) plane of the ITO structure can be noticed. The degree of crystallinity is lower when compared to the samples starting from 0.1 M ITO solution because the 0.25 M ITO solution is leading to the formation of thick films that require a longer time to remove the solvent. The removal of the solvent retards the crystallization of the films, and therefore the ITO 0.25 M films are not well-crystallized.

The optical properties of the films were studied by spectroscopic ellipsometry in the 350–800 nm spectral range. The ellipsometric measurements were fitted with three layer model: surface roughness layer/ITO film/substrate. The roughness layer was modelled by EMA (50 % voids + 50 % ITO film) and the ITO film was fitted with a Cauchy model in the transparency region to find out the thicknesses of the film and of SiO_2 layer between the substrate and film (in the cases of Si and $\text{SiO}_2/\text{glass}$ substrates).

From the best fit the thickness layers were obtained (see also Table 1). The thickness of SiO_2 buffer layer, measured on a bare substrate without film was 45.6 nm, a value in good agreement with SiO_2 layer measured by SEM. It can be observed that the thickness of the ITO films:

- increases with the sol concentration of ITO. The thicknesses of the 0.25 M ITO five layers films on all three substrates are higher than that of 0.1 M ITO ten layers films. This is very important information for the conductivity measurement.

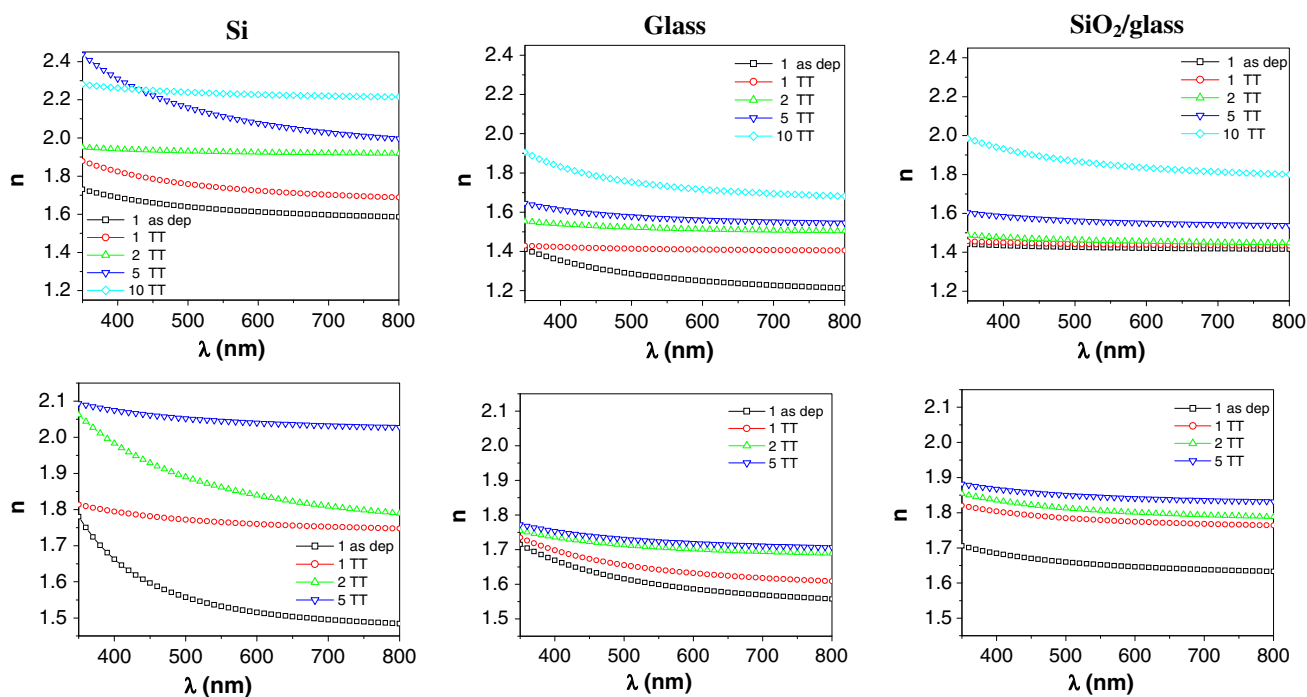


Fig. 9 Refractive index (n) dispersion of ITO films deposited on Si, glass and $\text{SiO}_2/\text{glass}$ from 0.1 M (*first row*) and, respectively, 0.25 M (*second row*) sol concentrations (*as dep* as deposited, *TT* thermally treated, 1–10 the number of layers)

- depends on the substrate; when SiO_2 buffer layer is present the ITO films are thicker.

The deposition number has a smaller effect on ITO films thickness in the case of diluted solution (0.1 M). This can be related to the film densification that occurs as a result of the thermal annealing after each deposition. Accordingly, each additional deposition causes mainly a decrease in the porosity of the ITO film rather than a significant increase of the thickness.

The refractive index dispersia (n) for all samples were determined from the best ellipsometric fit (Fig. 9).

For both substrates and solution concentrations refractive index increases with the number of layers and depends on the ITO molar concentration and substrate. All samples exhibit a very weak absorption (the extinction coefficient is practically zero) from visible to near-IR range.

With increasing of refractive index, reflection losses increases and transparency decreases. For transparent films with refractive indices varying between ~ 1.6 and 2.2, the reflection losses at normal incidence on the films is of the order of ~ 5 –14 %, so the transmission lowers from 90 to 76 %. For solar cell application we tried to obtain films with high transmission values, thus means small refractive index. To this end the sol–gel method is a suitable one, because we can model the proprieties of the films (e.g., refractive index) changing the ITO molar concentration, number of layers or the substrate type. Moreover the sol–

gel method is known to produce films with lower refractive indices than other methods due to the intrinsic porosity of the films associated with this technique.

The transmission of ITO sol–gel films was measured by ellipsometry in the range of 250–800 nm (Fig. 10) and it was found that all values are over 90 % for one layer films on both substrates (glass and $\text{SiO}_2/\text{glass}$) and decrease until 80 % for ten layers 0.1 M ITO films, respectively five layers 0.25 M ITO films, due to the reasons discussed above.

On the other hand a good conductivity can not be obtained for films with low number of layers, because it is not possible to obtain a high enough carrier concentration (N_D) and low enough resistivity (ρ). We attribute this effect to the high porosity of the films obtained after only 1–2 layers deposition. Thus we have focused on the study of the electrical properties for samples with ten (0.1 M ITO) and five (0.25 M ITO) layers (see Table 1). The concentration of the sol from which the samples are deposited has also significant influence. Lower sol concentration leads to the diminishing of the resistivity, independent of the substrate type. The most promising results were obtained for films with ten layers obtained from solution of 0.1 M concentration, deposited on glass and $\text{SiO}_2/\text{glass}$. These samples exhibited high carrier concentration and relatively low resistivity, but also a high recombination rate. It is very clear that the number of layers plays a crucial role both in transmission and in the electrical parameters.

Fig. 10 Transmissions of the ITO films: **a** 0.1 M ITO/glass; **b** 0.1 M ITO/SiO₂/glass; **c** 0.25 M ITO/glass; **d** 0.25 M ITO/SiO₂/glass (*as dep* as deposited, *TT* thermally treated, 1–10 the number of layers)

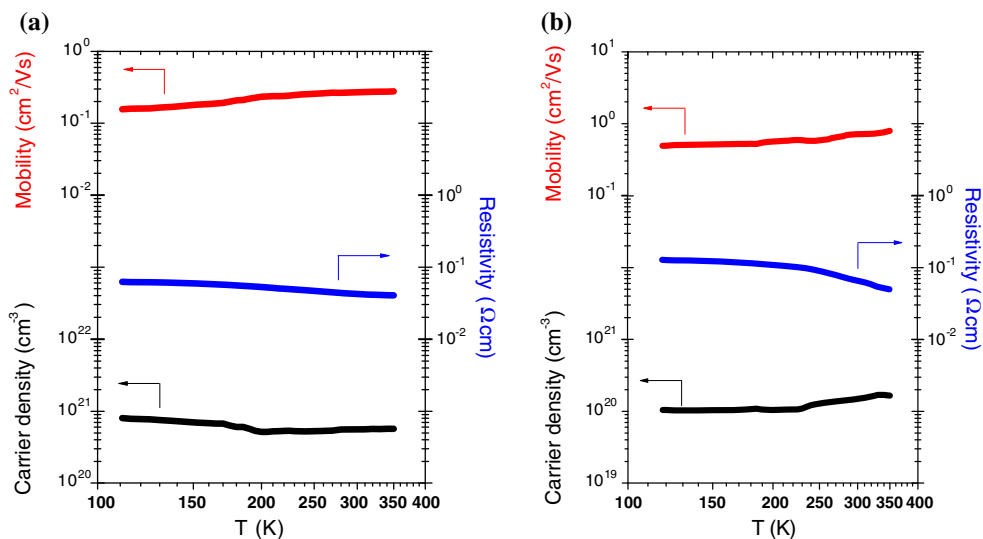
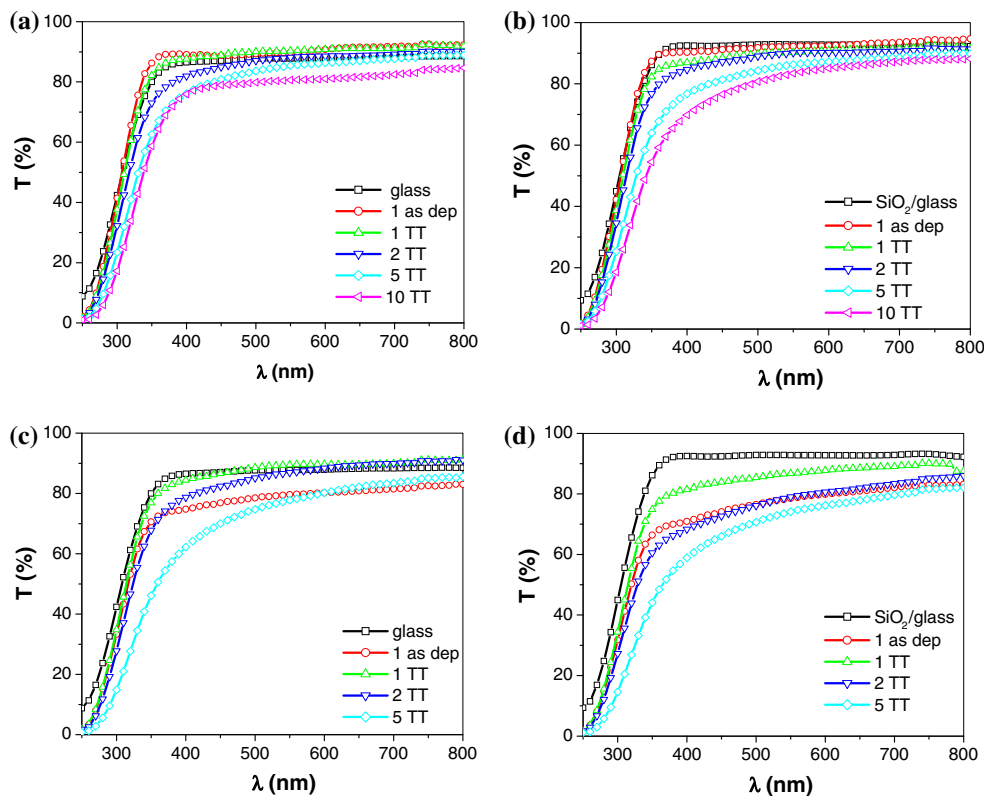


Fig. 11 Hall measurement with the temperature variation ($\Delta T = 110\text{--}350$ K) for 0.1 M ITO films with ten layers on SiO₂/glass (**a**) and glass (**b**)

Hall measurements were carried out for 0.1 M ITO sol-gel films with ten layers. The samples that gave the most promising results at room temperature (concentration 0.1 M, ten layers, glass and SiO₂ covered glass) were also measured at variable temperature between 110 and 350 K—Fig. 11.

Both samples exhibited typical semiconductor behavior where resistivity decreased with increasing temperature.

For the sample deposited on SiO₂ covered glass substrate, carrier concentration was generally flat over the temperature range used. There is also evidence of background noise especially at lower temperatures. The sample deposited on glass registers a slight increase in both carrier concentration and mobility with temperature.

A decrease in resistivity takes place between 280 and 300 K, dominated by the sudden increase in carrier

concentration. At high temperature, the thermally generated intrinsic carriers outnumber the dopants and carrier concentration increases with temperature.

The larger crystallites may enhance the conductivity of ITO films due to fewer grain boundaries [38].

4 Conclusions

Continuous and homogeneous films were deposited on three different substrates (glass, SiO₂/glass and silicon) by dip-coating method from 0.1 and 0.25 M sol concentrations. The influence of solution concentrations, number of layers and type of substrate on the structural, morphological, optical and electrical properties of the ITO films was studied by XRD, SEM, AFM, SE, optical transmission and electrical measurements. ITO structure was found on all studied films, but with different degrees of crystallinity, function of the number of depositions (which in its turn is correlated with the number of thermal treatments) and sol concentration. The smoothest surface with the smallest variation in thickness along the film was observed on Si substrate, while the SiO₂/glass substrate results in the roughest film surface. As general remark, the ITO films obtained from 0.1 M solution with ten layers deposited on glass and SiO₂/glass present the best TCO characteristics, namely transmission around 90 % and the carrier concentration around 10²⁰ cm⁻³. The results of these experiments demonstrated the possibility to select a suitable substrate, sol-concentration and number of layers deposition for a certain application.

Acknowledgments This work was supported by the Romanian PN-II-ID-PCE-2011-3-0446 Project and by EU (ERDF) and Romanian Government that allowed for acquisition of the research infrastructure under POS-CCE O 2.2.1 Project INFRANANOCHEM—Nr. 19/01.03.2009.

References

- Lunt RR, Bulovic V (2011) *Appl Phys Lett* 98:113305
- Tien WC, Chu AK (2014) *Sol Energ Mater Sol C* 120:18–22
- Furukawa K, Terasaka Y, Ueda H, Matsumura M (1997) *Synth Met* 91(1–3):99–101
- Li Z-H, Cho E-S, Kwon SJ (2010) *Appl Surf Sci* 257(3):776–780
- Celik E, Aybarc U, Ebeoglugil MF, Birlik I, Culha O (2009) *J Sol-Gel Sci Technol* 50:337–347
- Sierros KA, Morris NJ, Kukureka SN, Cairns DR (2009) *Wear* 267(1–4):625–631
- Ahn MH, Cho E-S, Kwon SJ (2011) *Appl Surf Sci* 258:1242–1248
- Houng B, Lin SL, Chen SW, Wang A (2011) *Ceram Int* 37:3397–3403
- Lee CJ, Lin HK, Li CH, Chen LX, Lee CC, Wu CW, Huang JC (2012) *Thin Solid Films* 522:330–335
- Manavizadeh N, Boroumand FA, Asl-Soleimani E, Raissi F, Bagherzadeh S, Khodayari A, Rasouli MA (2009) *Thin Solid Films* 517:2324–2327
- Song S, Yang T, Liu J, Xin Y, Li Y, Han S (2011) *Appl Surf Sci* 257:7061–7064
- Stroescu H, Anastasescu M, Preda S, Nicolescu M, Stoica M, Stefan N, Kampylafka V, Aperathitis E, Modreanu M, Zaharescu M, Gartner M (2013) *Thin Solid Films* 541:121–126
- Wasa K, Hayakawa S (1991) *Handbook of sputter deposition technology*. Noyes Publications, NJ
- Facchetti A, Marks TJ (2010) *Transparent electronics: from synthesis to applications*. Wiley, New York
- Gunley DS, Hosono H, Paine DC (2010) *Handbook of transparent conductors*. Springer, New York
- Rozati SM, Ganj T (2004) *Renew Energy* 29(10):1671–1676
- El Rhaleb H, Benamar E, Rami M, Roger JP, Hakam A, Ennaoui A (2002) *Appl Surf Sci* 201(1–4):138–145
- Bisht H, Eun H-T, Mehrtens A, Aegerter MA (1999) *Thin Solid Films* 351:109–114
- Madhi I, Saadoun M, Bessais B (2012) *Procedia Eng* 47:192–195
- Mbarek H, Saadoun M, Bessais B (2006) *Mater Sci Eng C* 26(2–3):500–504
- Meng L-J, Gao J, Silva RA, Song S (2008) *Thin Solid Films* 516:5454–5459
- Zhinong Y, Yuqiong L, Fan X, Zhiwei Z, Wei X (2009) *Thin Solid Films* 517:5395–5398
- Okuya M, Ito N, Shiozaki K (2007) *Thin Solid Films* 515:8656–8659
- Fallah HR, Varnamkhasti MG, Vahid MJ (2010) *Renew Energy* 35:1527–1530
- Senthilkumar V, Vickraman P, Jayachandran M, Sanjeeviraja C (2010) *Vacuum* 84:864–869
- Stoica TF, Stoica TA, Vanca V, Lakatos E, Zaharescu M (1999) *Thin Solid Films* 348:273–278
- Stoica TF, Stoica TA, Zaharescu M, Popescu M, Sava F, Popescu-Pogriion N, Frunză L (2000) *J Optoelectron Adv Mater* 2:684–688
- Alam MJ, Cameron DC (2000) *Thin Solid Films* 377:455–459
- Stoica TF, Gartner M, Losurdo M, Teodorescu VS, Blanchin M, Stoica T, Zaharescu M (2004) *Thin Solid Films* 455–456:509–512
- Biswas PK, De A, Dua LK, Chkoda L (2006) *Appl Surf Sci* 253:1953–1959
- Beaurain A, Luxembourg D, Dufour C, Koncar V, Capoen B, Bouzaoui M (2008) *Thin Solid Films* 516:4102–4106
- Valencia HY, Moreno LC, Ardila AM (2008) *Microelectron J* 39:1356–1357
- Prodi-Schwab A, Luthe Th, Jahn R, Herbig B, Lobmann P (2008) *J Sol-Gel Sci Technol* 47:68–73
- Solimana A, Zayeda MK, Alamria SN, Al-Dahoudib N, Aegerter MA (2012) *Mater Chem Phys* 134:127–132
- Liu J, Wu D, Zhang N, Wang Y (2010) *Rare Met* 29(2):143–148
- Kittel C (1996) *Introduction to solid state physics*. Wiley, New York
- Van Meerssche M, Feneau-Dupont J (1984) *Introduction à la cristallographie et à la chimie structurale*. Editions Peeters, Leuven
- Su C, Sheu TK, Chang YT, Wan MA, Feng MC, Hung WC (2005) *Synth Met* 153:9–12